SolarPACES 2024, 30th International Conference on Concentrating Solar Power, Thermal, and Chemical Energy Systems

Analysis and Simulation of CSP and Hybridized Systems

https://doi.org/10.52825/solarpaces.v3i.2445

Published: 26 Jan. 2026

Hydrogen Production by Means of Small-Scale Multi-Tower CSP Plants Based on sCO_2 Power Cycles and Solid Oxide Electrolysers

SolarPACES 2024

Simone Girelli[1], Marco Ficili[1], Dario Alfani[1,*], Paolo Colbertaldo[1], Ettore Morosini[1], Giancarlo Gentile[1], Marco Astolfi[1], Marco Binotti[1], and Paolo Silva[1]

[1]Politecnico di Milano, Energy Department, Italy

*Correspondence: Dario Alfani, dario.alfani@polimi.it

Abstract. Concentrated Solar Power can play a relevant role in the decarbonization of the energy sector as it can integrate cost-competitive Thermal Energy Storage, allowing for dispatchable electricity generation. Furthermore, there has been a notable increase in hydrogen demand over the past decade, with most of it being produced using fossil fuels, entailing a large contribution in CO_2 emissions. In this context, the Italian Research Project of National Relevance MUSIC aims to demonstrate the potential of small-scale multi-tower concentrated solar power plants with sodium as heat transfer fluid that are thermally and electrically integrated with a solid oxide electrolyzer to produce green hydrogen and electricity. The objective of this study is to evaluate the performance of a 2 MW_{el} plant for hydrogen production located in Sicily, Italy, by means of numerical models specifically developed to accurately simulate the plant components. A parametric analysis on the number of modules has been carried out and the results show that plants characterized by a smaller field achieve higher optical efficiencies and a lower auxiliary consumption of the HTF pump, at the expenses of lower receiver and piping thermal efficiencies. A maximum yearly solar to hydrogen efficiency of 16.6% was achieved, which largely exceeds the one of conventional PV + PEM systems, proving the potential of the technology.

Keywords: Small-Scale CSP, Multi-Tower, sCO_2, Solid Oxide Electrolyser

1. Introduction

A large increase in the shares of renewables is expected in the next future to reach net zero emissions in Europe by 2050. In this context, Concentrated Solar Power (CSP) plants are considered a key technology for decarbonization thanks to the use of cost-competitive thermal energy storage (TES), enabling the production of renewable dispatchable electricity, a critical issue in an energy market characterized by a high percentage of non-programmable energy sources. In addition, hydrogen is also seen as a potential alternative fuel to decarbonize the industrial and the transport sector and so its demand is expected to rise in the near future [1]. In 2022, 96% of hydrogen production in Europe was based on natural gas [1], resulting in relevant CO_2 emissions, further increasing the need for green hydrogen production technologies.

Under this framework, the MUSIC (MUlti-tower small-scale concentrating Solar power plants based on efficient and flexible sCO_2 cycles to provide dispatchable electricity and hydrogen production for the Italian Context) project aims to study the potential of flexible small-scale multi-tower CSP plants with sodium as heat transfer fluid (HTF) that are thermally and electrically integrated with a supercritical CO_2 cycle (sCO_2) and a solid oxide electrolyzer (SOE) for the combined production of electricity and green hydrogen. The integration between CSP and high-temperature electrolysis has already been proposed by Mastropasqua et al. [2] and has also been studied in EU projects such as SOPHIA [3]. Nevertheless, in literature there are currently no studies investigating the use of small-scale modular towers for the production of hydrogen and electricity. As 3rd generation solar receivers are potentially able to reach temperatures higher than 700°C, power blocks using sCO_2 as working fluid represent an ideal solution to increase efficiency and reduce cost of future CSP plants, as already investigated by several EU projects (sCO_2-Flex [4], Powder2Power [5]) and US (G3P3 [6]).

Additionally, multi-tower solar fields allow to increase the optical efficiency of CSP systems, mainly thanks to their limited size, and have a large potential for cost reduction through component standardization as proved by the activities of Vast [7]. Modular solar fields would also reduce issues related to visual impact and social acceptance, factors that previously caused the stop of several CSP projects in Italy [8]. Therefore, the objective of this work is to carry out a preliminary evaluation of a sCO_2 based CSP + SOE plant to produce green hydrogen, including a comparison with other competitive technologies representing the state-of-the-art of hydrogen production from solar energy (i.e. photovoltaic (PV) coupled to proton exchange membrane (PEM) electrolyzer plants). To address this task, numerical models for the design and simulation of all the main components have been developed to accurately compute their performance and to account for their reciprocal interactions.

2. System description

The present work investigates a 2 MW_{el} CSP plant based on a series of small towers equipped with billboard receivers with sodium, one of the most promising HTF for next-generation high-temperature receivers [9]. A direct 2-tank TES has been assumed for simplicity, since the choice of a difference storing medium would influence only the results of a complete tecno-economic optimization of the technology, which is not proposed in this work. The sCO_2 power block exploits the thermal power generated from the solar field to provide electricity and superheated steam to the SOE. Steam is produced from water at ambient temperature by exploiting the thermal power rejected from the sCO_2 power block without penalizing its performance The plant scheme is reported in **Figure 1**.

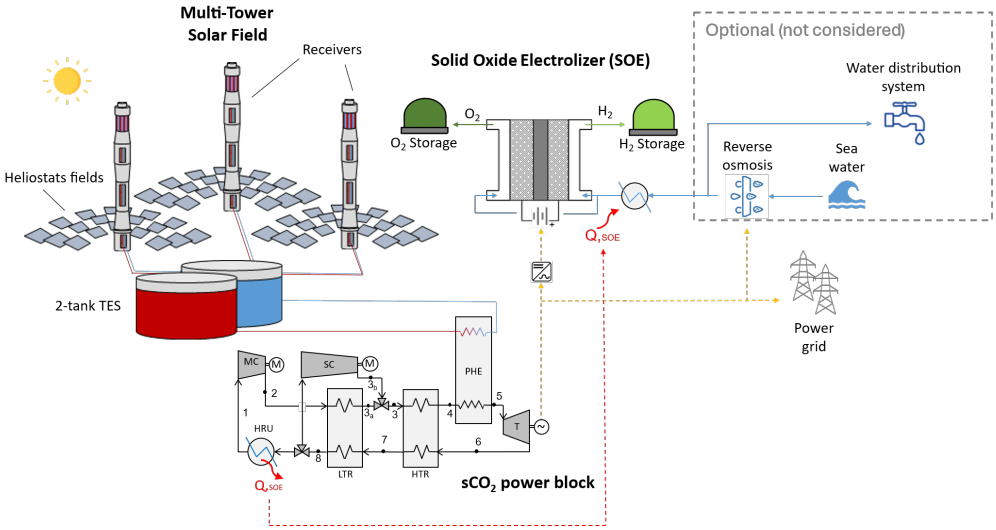

Figure 1. *MUSIC plant scheme*

3. Methodology

The plant is designed in Vittoria, Sicily, Italy (37.21°N, 14.46°W, 5.45 kWh/m^2/day), considering a solar multiple (SM) of 3 and 13 hours of storage, based on the results proposed in [10].

Each component of the system is simulated using dedicated numerical models, and the results are used to compute the sun-to-hydrogen efficiency ($\eta_{solar\ 2\ H_2}$), as defined by Eq. (*1)* as the product of solar field optical efficiency, receiver and piping thermal efficiency, efficiency of the power block and fuel cell performance:

$$\eta_{solar\ 2\ H_2} = \eta_{opt} \cdot \eta_{th,rec} \cdot \eta_{th,piping} \cdot \eta_{PB} \cdot \eta_{SOE} \quad (1)$$

The solar field layout, its optical efficiency and the heat flux maps on the receiver as function of the sun position are generated with SolarPILOT [11]. The obtained receiver heat flux maps are then used to compute its thermal efficiency with an in-house MATLAB model [10]. Subsequently, the piping system interconnecting each tower to the storage tank and to the power block is designed and simulated using a MATLAB numerical model able to predict the piping thermal losses and the consumption of the circulation pump. Lastly, the sCO_2 cycle performance has been computed using MATLAB + REFPROP V9.1, while the SOE is simulated in Aspen Plus. A set of design choices has been consolidated considering the strong interaction between the different components. Firstly, the solar fields are designed according to the procedure reported in detail in section 3.1. After that, the HTF temperature range is optimized, considering the trade-off between the receiver and piping thermal efficiency and the power block + SOE subsystem efficiency while considering a minimum temperature difference between the sodium and the sCO_2 of 20°C The sCO_2 power block is sized to fulfil the electrical load of the SOE, and thus the definition of the system optimal design is carried out considering the thermal-to-H_2 efficiency, as reported in Equation (**2**) and not the conventional cycle efficiency.

$$\eta_{th\ 2\ H_2} = \frac{\dot{m}_{H_2} \cdot LHV_{H_2}}{\dot{Q}_{in,PB}} = \eta_{PB} \cdot \eta_{SOE} \quad (2)$$

Finally, the thermal losses and pump auxiliary consumption for the circulation of the HTF in the piping system is evaluated after assuming the arrangement of the modules. The material chosen for both the piping and the receiver tubes is Inconel 617, which is suggested for high temperature applications [12].

Four different plants are considered in this work: three modular plants (characterized by 15, 5 or 3 modules) and a single-tower plant. The total design power of the solar field has been evaluated assuming a first-guess value of the power block efficiency at 0.4, leading to a total power of 15 MW_{th} delivered to the HTF. In the case of modular plants, the thermal power on each module is computed by homogeneously split the overall thermal input within the different modules.

3.1. Solar field and receiver

The solar fields are generated considering a flat plate receiver, 2 m x 2 m heliostats in analogy with the Jemalong plant [13], a DNI of 900 W/m^2 at solar noon at summer solstice and including a receiver thermal loss of 140 kW/m^2 according to a preliminary evaluation done by simulating some cases with the model described in [10]. A radial stagger layout is employed for the heliostat field as it achieved the best performance in terms of optical efficiency in a set of preliminary simulations. For all cases, the tower height is computed as a function of the design HTF thermal power through a linear regression based on small-scale solar tower CSP plants data available in literature [14], resulting in the correlation of Eq. (3).

$$h_{tower}[\text{m}] = \dot{Q}_{HTF}[\text{MW}] \cdot 6.024 + 29.72 \qquad (for: \dot{Q}_{HTF} < 20\ MW_{th}) \quad (3)$$

The receiver size is defined assuming an aspect ratio of 1 [15] and minimizing the capital cost of the whole solar field, considering the trade-off between receiver and heliostats costs (i.e. with a techno-economic trade-off between the optical and thermal losses). In particular, the standard SolarPILOT heliostat cost of 140 \$/m^2 and a receiver cost of 135 \$/kW of incident power are assumed [10]. In order not to overcome the limit of 2 MW/m^2 on the heat flux for a sodium based receiver [16], the 'Image size priority' aim strategy was adopted and the minimum image offset was iteratively decreased until the limit was respected. The receivers were tilted downward by 25° and oriented facing north to maximize the field optical efficiency.

The receiver thermal efficiency and the HTF pressure drops are evaluated with a steady-state three-dimensional model implemented in MATLAB and described in [10]. Receiver part-load performance, required for the annual analysis, is obtained simply by scaling the flux map between 20% and 110% of the design value, as receiver efficiency is marginally influenced by the heat flux distribution [17]. For all the considered cases, 2 panels and 2 flow paths are considered. Differently, the receiver tubes diameter and thickness are chosen among commercial standard dimensions aiming at the best trade-off between thermal efficiency and pressure loss through the maximization of the design net power to the receiver, $\dot{Q}_{net}$, as in Eq. (4), equal to the thermal power delivered to the HTF reduced by the fictitious thermal power necessary to operate the HTF circulation pump, computed assuming a thermal-to-power efficiency (η'_{PB}) of 40%:

$$\dot{Q}_{net} = \dot{Q}_{rec} - \frac{\dot{W}_{pump,rec}}{\eta'_{PB}} \tag{4}$$

3.2. Piping system

A numerical tool was developed in MATLAB for the design of the piping system of modular CSP power plants and the computation of its thermal and pressure losses. The model represents the piping as a graph, wherein all pipe junctions are represented by nodes and graph edges represent each pipe section. The model computes both concentrated and distributed pressure losses, computes the thickness of all insulation layers using the method proposed in [18], assuming a temperature difference between the ambient and the external surface of 2°C, as suggested in [10] and computes the thermal losses accordingly. Additionally, expansion loops, similar to those of the Jemalong power plant [13], are considered to accommodate the axial thermal expansion of the piping.

For simplicity, the modules are arranged in parallel rows with the TES system in the middle as changing the layout of the modules did not lead to significant changes in performances. Once the position of each module is fixed, the tool is employed to identify the optimal sodium velocity with the same procedure explained for the receiver (Eq. (4)), but referring to the piping system and eventually design each pipe section accordingly. The pump consumption is computed assuming the use of a single HTF circulation pump station and the adoption of valves to balance the pressure drops and mass flow rates in each branch of the piping system. Consequently, the pump must guarantee the head related to the branch featuring the highest pressure drops After the geometry of the piping is fully defined, its off-design performance is evaluated for each thermal load in off-design by modifying the sodium mass flow rate accordingly while the pumping station hydraulic efficiency has been assumed constant considering the use of different variable speed pumps in parallel.

3.3. Power block and SOE

The numerical tool previously described in [19], [20] is used for the simulation of the power block considering the main assumptions reported in Table 1, while the SOE performance is numerically derived with a model adapted from the one already presented in [21].

Table 1. *sCO_2 power cycle base assumptions*

Parameter	Value	Parameter	Value
Compressor isentropic efficiency	80%	PHE pressure losses	1%
Turbine isentropic efficiency	85%	HRU pressure losses	1%
LTR pressure losses	0.5%	HTR pressure losses	0.5%
Generator efficiency	98.5%	Motor efficiency	97%
Maximum pressure	250 bar	Ambient temperature	35 °C

Four cycle architectures have been preliminary analyzed: the simple recuperative cycle, the recompressed cycle, the recompressed cycle with intercooling and the partial cooling cycle. The simple recuperative cycle has been discarded due to its poor thermodynamic efficiency compared to the other architectures, which lead to less efficient hydrogen production. Differently, the recompressed cycle with intercooling and the partial cooling cycles showed poor $\eta_{th\,2\,H_2}$ due to their lower temperature of heat release compared to the recompressed cycles and are thus not able to fulfill SOE thermal needs and require an additional electric heater leading to a significant efficiency penalization. In conclusion, only the recompressed cycle has been then considered in this work and the optimization of the system is carried out based on the thermal-to-hydrogen efficiency thus considering simultaneously both the power block and SOE efficiency, which also includes the additional electric heater consumption required in cases where the heat recovery from the power block is not sufficient to fulfill the low temperature heat demand of the SOE.

The performance of the cycle has been analyzed by varying parametrically the parameters reported in Table 2 and optimizing for each investigated case the pinch point temperature difference of the low temperature recuperator (LTR) to optimize the hydrogen production efficiency. The maximum temperature of sodium was capped at 740 °C to respect both the limit temperature of sodium [9] and of Inconel 617 [12], resulting in a cycle maximum temperature limited to 720°C.

Table 2. *sCO_2 power cycle optimization parameters*

Parameter	Range	Step
Minimum temperature	[40 °C - 70 °C]	10°C
Maximum temperature	[660 °C – 720°C]	10°C
HTR pinch point ΔT	[5 °C – 65 °C]	2.5°C
LTR pinch point ΔT	[5 °C – 65 °C]	-

The SOE plant is composed of multiple modules, each consisting of several high-temperature electrolysis stacks and related balance of plant (heat exchanger, separation units, recycle blowers, etc.). Inlet water is pre-heated, evaporated, and superheated up to 120°C using low-temperature external heat and then sent to the SOE module, where the inlet streams (steam and air) are further heated up exploiting regenerative exchange and external high-temperature heat supply and finally enter the solid oxide cell stack. The system is modelled and simulated using Aspen Plus, assuming the use of conventional (YSZ-based) cells and stack operation at 700°C and 1 atm, with 70% steam utilization factor. In the overall CSP+SOE analysis, the integration entails the use of waste heat from the heat rejection unit of the sCO_2 cycle to the water evaporation section, whereas electricity is provided to the SOE module for high-temperature heaters, stacks, and auxiliaries.

It is assumed that the power block and SOE are always operated at full load whenever there is sufficient thermal power from the HTF, consequently, their part load behavior has not been considered. It is also assumed that a variable speed fan is employed in the heat rejection unit (HRU) to keep a constant minimum temperature of the cycle regardless of the ambient

temperature, allowing the power block to work always on design conditions, without penalizing the heat rejection to the SOE.

4. Results

The main results of the solar fields optimization are reported in Table 3, where the values reported in the table below refers to the single solar field.

Table 3. *Solar field design optimization results, the receiver and piping thermal efficiencies are computed for the optimal HTF temperature*

	15 Modules	**5 Modules**	**3 Modules**	**1 Module**
Module target power to HTF	1 MW	3 MW	5 MW	15 MW
Module effective power to the HTF	1.02 MW	2.97 MW	4.95 MW	14.83 MW
Number of heliostats	445	1302	2194	6966
Design η_{opt}	75.8 %	75.1 %	72.9 %	67.5 %
Receiver width	1.12 m	1.82 m	2.21 m	3.64 m
Tower height	35.7 m	47.8 m	59.8 m	120.1 m
Design $\eta_{th,rec}$	86.5 %	87.3 %	88.6 %	89.7 %
Design $\eta_{th,piping}$	96.5 %	97.5 %	97.8 %	99.2 %
Design $\eta_{solar\ 2\ th}$	63.2 %	63.9 %	63.1 %	60.0 %
Design $\dot{W}_{pump}$	16.8 kW	21.7 kW	32.3 kW	85.6 kW
Design Hot / cold piping losses	174/141 W/m	191/155 W/m	206/168 W/m	242/202 W/m

As expected, the modular fields show a higher optical efficiency compared to the single tower case thanks to their smaller size, which entails a reduction of cosine, attenuation and spillage losses both in design and for all the sun positions as visible in Figure 2. To limit the computational time on the large set of case studies analyzed, the number of iterations between the optical and thermal models was limited, thus implying a small deviation between target and obtained power.

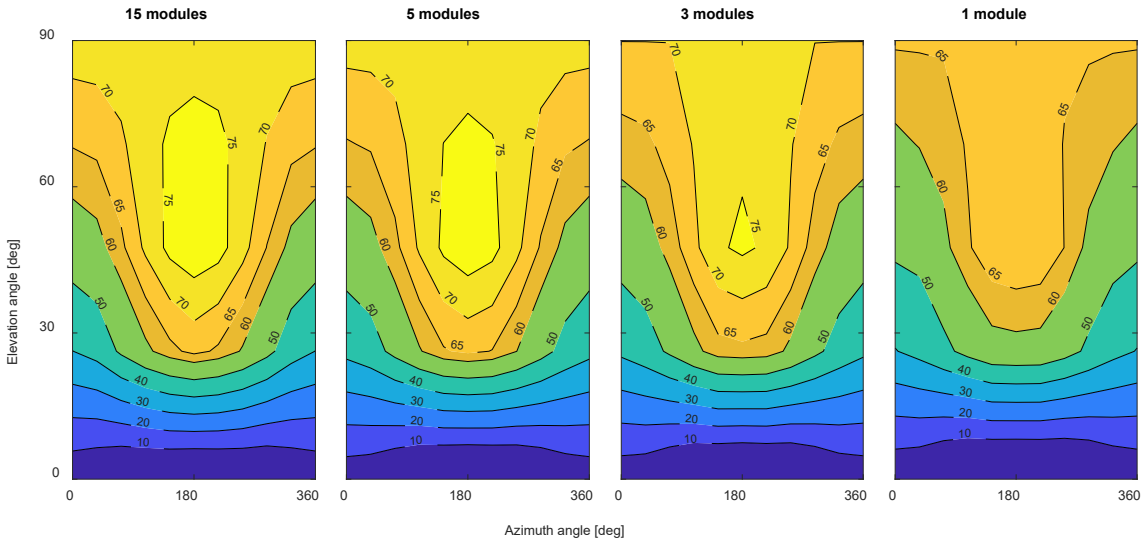

Figure 2. *Optical efficiency as a function of the elevation angle and azimuth angle for different numbers of modules*

Both the receiver and piping exhibit lower thermal efficiency for smaller modules, as reported in Table 3 and Figure 3. Larger fields produce a more uniform heat flux distribution of the receiver surface thanks to the chosen aiming strategy, with consequent higher average flux for the same peak flux and thus higher thermal efficiency. On the other hand, modular plants are penalized in term of piping thermal efficiency due to their longer piping network. Plants characterized by smaller modules exhibits higher specific thermal losses per unit length (as reported in Table 3) due to the higher piping cross-section, which leads to higher external surface areas. However, the reduction in the piping length is greater than the increase of the specific losses, which in the end results in higher piping thermal efficiency. In contrast, the overall pressure drop decreases with the number of modular fields as the pressure drop in the piping system is less significant than the drop inside the receiver, which is higher for the larger receivers. Consequently, the modular solution also allows to reduce the consumption related to the circulation of the sodium ($\dot{W}_{pump}$) which decreases by a factor of 4.1 from single module plant to a 15-module plant

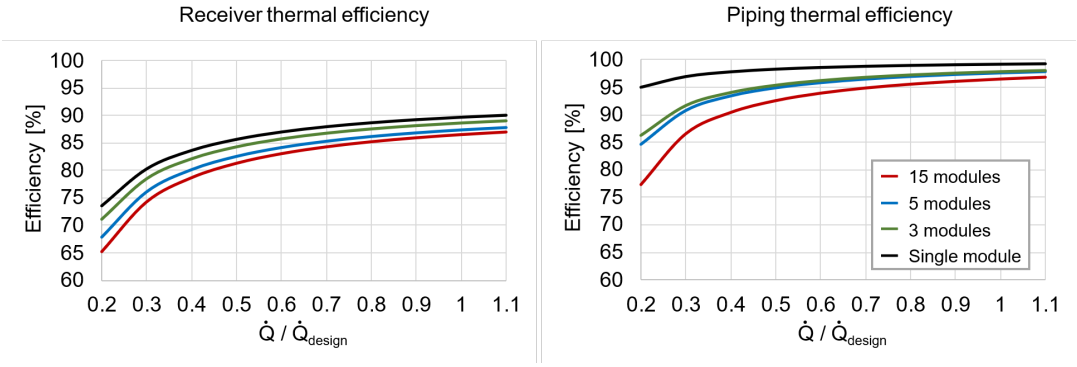

Figure 3. *Receiver and piping thermal efficiency at different thermal inputs*

The results of the trade-off between the receiver and piping thermal efficiency and PB + SOE efficiency as a function of the cycle maximum temperature at design conditions are reported in Figure 4 for the 15 modules case. As expected, the higher the maximum temperature, the higher the sCO_2 + SOE efficiency and the lower the receiver + piping efficiency. However, since the receiver + piping efficiency reduction is limited, the optimal overall efficiency is reached at the highest investigated temperature. The same trend applies to all cases.

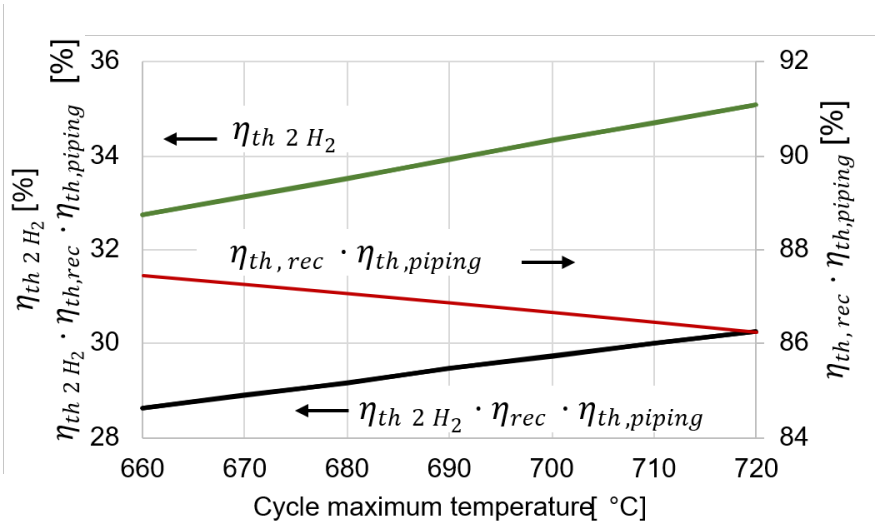

Figure 4. *Effect of TIT on thermal-to-hydrogen, receiver, piping and total efficiency for the 15 modules case*

Consequently, for all the cases, the maximum sodium temperature was fixed to 740 °C, leading to a $\eta_{th\ 2\ H_2}$ optimal value of 35.1 %. As evidenced by the optimal operating parameters detailed in Table 4, the optimal minimum temperature of the cycle is significantly higher than the typical ambient temperature, because a lower minimum temperature would decrease the heat released by the cycle, thus penalizing the overall efficiency due to the increase in the electrical heater consumption.

Table 4. *Optimized parameters for the sCO_2 power cycle*

Parameter	Value
Minimum temperature	60 °C
Maximum temperature	720°C
HTR ΔT pinch point	10 °C
LTR ΔT pinch point	7.9 °C

Based on these results a preliminary annual simulation on an hourly basis was carried out to compute the yearly hydrogen production and the yearly average plant efficiency. It is assumed that for an available thermal input to the receiver lower than 20%, the solar field is completely defocused, while at high irradiation the heliostats are partially defocused to limit the actual thermal input at maximum 110% of the nominal one.

Results are reported in Table 5, where it is possible to notice that, referring to the nominal solar to H2 efficiency, the 5-module plant shows the best performance whereas the single module layout is identified as the least efficient solution. When considering the annual efficiency, the 5-module case remains the most promising configuration, overperforming the 3 module configuration (penalized by higher optical losses) and the 15 module configuration (penalized by higher thermal losses). Additionally, the results showed that all the modular solutions have higher annual efficiencies compared to the single-field case, with a 4.6%, 7% and 6% increase for the 15, 5 and 3-module layout, respectively, proving that the benefit of an improved optical efficiency is more relevant than the drawback of a lower thermal efficiency of the receiver and piping.

The system achieves significantly higher efficiencies than more conventional solutions, such as PV + PEM: those plants can reach annual sun to H2 efficiencies around 12% in the optimal case where the PV and the PEM are directly linked and operate at the same voltage, but is usually limited to 2 - 6% for conventional systems [22]. On the other hand, the performance of the investigated system is consistent with the hybrid CSP + SOE plant based on parabolic dish and micro gas turbines proposed in literature by Mastropasqua et al, which can achieve yearly efficiencies in the range of 13% (standard performance of components) to 19% (improved components efficiency) [2].

Table 5. *Overall sun to H_2 design and annual efficiency of the plant*

	15 Modules	5 Modules	3 Modules	Single module
Design solar-to-H_2 efficiency	22.2%	22.5%	22.2%	21.8%
Annual optical efficiency	57.6%	57.5%	55.9%	51.3%
Annual receiver efficiency	84.6%	85.4%	86.9%	88.0%
Annual piping efficiency	95.1%	96.5%	96.8%	98.8%
Annual sun to H_2 efficiency	16.2%	16.6%	16.4%	15.5%
Capacity factor	55.8%	56.0%	55.8%	53.8%

5. Conclusion and future works

This work presents a preliminary evaluation of a modular CSP plant based on sodium tower receivers and a sCO_2 power cycle, thermally and electrically integrated with a SOE for green hydrogen production. Various numerical models were developed and integrated to simulate and optimize each component of the plant, considering also their mutual interactions. The off-design performances of the main components were eventually computed and used in a preliminary annual simulation to evaluate the yearly efficiency of the plant in realistic operative conditions

Results showed that modular plants characterized by a smaller field allow to achieve greater optical efficiencies and lower pumping power consumption but are characterized by lower thermal efficiencies of both the receiver and the piping system. In particular, the 5x3 MW_{th} plant exhibits both the highest design point efficiency (22.5%) and the highest yearly efficiency ($\eta_{solar\ 2\ H_2,annual}$ = 16.6%) thanks to its better annual optical efficiency even though similar performance are achieved by the other modular options. These results prove that the adoption of modular plants can lead to better efficiency than single tower conventional systems, while also having a lower visual impact and potential for cost reduction which will be evaluated in future works. The achieved performance is significantly higher than conventional PV + PEM systems (<10%), highlighting the potential of the proposed technology as an alternative solution for green hydrogen production from solar energy.

Future works will focus on techno-economic analysis to optimize also the size of the system including the nominal power of the sCO2 plant and SOE, the solar multiple and hours of storage and evaluate the results on the base of the levelized cost of hydrogen. Additionally, future studies will focus on the development of operational strategies able to maximize the profitability of the system under different scenarios characterized by different prices of electricity and hydrogen.

Data availability statement

Data will be made available on request.

Author contributions

Simone Girelli: Software, Methodology, Formal analysis, Investigation, Visualization, Writing - Original Draft **Marco Ficili:** Software, Investigation **Dario Alfani:** Software, Conceptualization, Methodology, Writing - Review and Editing, **Paolo Colbertaldo:** Supervision, Writing – Review and Editing, **Ettore Morosini:** Writing – Review and Editing, **Giancarlo Gentile:** Software, **Marco Astolfi:** Supervision, Writing – Review and Editing **Marco Binotti:** Supervision, Writing – Review and Editing, **Paolo Silva:** Project administration, Funding acquisition, Supervision

Competing interests

The authors declare that they have no known competing financial interests or personal relationships that could have appeared to influence the work reported in this paper.

Funding

This study received funding from the European Union - Next-GenerationEU - National Recovery and Resilience Plan (NRRP) – MISSION 4 COMPONENT 2, INVESTIMENT N. 1.1, CALL PRIN 2022 PNRR D.D. 1409 14-09-2022 – (MUSIC) CUP N. D53D23003850006.

This study was carried out within the NEST - Network 4 Energy Sustainable Transition (D.D. 1243 02/08/2022, PE00000021) and received funding under the National Recovery and Resilience Plan (NRRP), Mission 4 Component 2 Investment 1.3, funded from the European Union - NextGenerationEU. This manuscript reflects only the authors' views and opinions, neither the European Union nor the European Commission can be considered responsible for them.

References

[1] European Comission, 'EU Hydrogen Strategy', europa.ue. Accessed: Aug. 16, 2024. [Online]. Available: https://energy.ec.europa.eu/topics/energy-systems-integration/hydrogen_en

[2] L. Mastropasqua, I. Pecenati, A. Giostri, and S. Campanari, 'Solar hydrogen production: Techno-economic analysis of a parabolic dish-supported high-temperature electrolysis system', *Applied Energy*, vol. 261, p. 114392, Mar. 2020, doi: 10.1016/j.apenergy.2019.114392.

[3] European Comission, 'Solar integrated pressurized high temperature electrolysis | SOPHIA Project', CORDIS | European Commission.

[4] 'sCO2-flex'. Accessed: Aug. 17, 2024. [Online]. Available: https://www.sco2-flex.eu/

[5] 'Powder2Power Project'. Accessed: Apr. 05, 2024. [Online]. Available: https://powder2power-project.eu/

[6] Sandia National Laboratories, 'G3P3 project'. Accessed: Apr. 05, 2023. [Online]. Available: https://energy.sandia.gov/programs/renewable-energy/csp/current-research-projects/gen-3-particle-pilot-plant-g3p3/

[7] 'Vast – Our Technology'. Accessed: Aug. 17, 2024. [Online]. Available: https://www.vast.energy/about-technology

[8] 'Strategia Energetica Nazionale 2017', MISE. Accessed: Aug. 17, 2024. [Online]. Available: https://www.mase.gov.it/comunicati/strategia-energetica-nazionale-2017

[9] G. Manzolini, G. Lucca, M. Binotti, and G. Lozza, 'A two-step procedure for the selection of innovative high temperature heat transfer fluids in solar tower power plants', *Renewable Energy*, vol. 177, pp. 807–822, Nov. 2021, doi: 10.1016/j.renene.2021.05.153.

[10] E. Morosini, G. Gentile, M. Binotti, and G. Manzolini, 'Techno-economic assessment of small-scale solar tower plants with modular billboard receivers and innovative power cycles', *J. Phys.: Conf. Ser.*, vol. 2385, no. 1, p. 012109, Dec. 2022, doi: 10.1088/1742-6596/2385/1/012109.

[11] M. J. Wagner and T. Wendelin, 'SolarPILOT: A power tower solar field layout and characterization tool', *Solar Energy*, vol. 171, pp. 185–196, Sep. 2018, doi: 10.1016/j.solener.2018.06.063.

[12] Z. Zhang, R. Ding, Q. Guo, C. Liu, and Y. Liu, 'Improving the microstructural stability and tensile properties of Inconel 617 superalloy at high temperature by stabilization of the γ′ phase', *Journal of Materials Research and Technology*, vol. 29, pp. 2991–2998, Mar. 2024, doi: 10.1016/j.jmrt.2024.02.058.

[13] 'Vast – Past Projects', Vast solar. Accessed: Aug. 20, 2024. [Online]. Available: https://www.vast.energy/past-projects

[14] 'Power Tower CSP Projects', NREL. Accessed: Aug. 20, 2024. [Online]. Available: https://solarpaces.nrel.gov/by-technology/power-tower

[15] T. Conroy, M. N. Collins, J. Fisher, and R. Grimes, 'Levelized cost of electricity evaluation of liquid sodium receiver designs through a thermal performance, mechanical reliability, and pressure drop analysis', *Solar Energy*, vol. 166, pp. 472–485, May 2018, doi: 10.1016/j.solener.2018.03.003.

[16] J. Coventry, C. Andraka, J. Pye, M. Blanco, and J. Fisher, 'A review of sodium receiver technologies for central receiver solar power plants', *Solar Energy*, vol. 122, pp. 749–762, Dec. 2015, doi: 10.1016/j.solener.2015.09.023.

[17] G. Gentile, G. Picotti, M. Binotti, M. E. Cholette, and G. Manzolini, 'A comprehensive methodology for the design of solar tower external receivers', *Renewable and Sustainable Energy Reviews*, vol. 193, p. 114153, Apr. 2024, doi: 10.1016/j.rser.2023.114153.

[18] A. M. Bonanos, M. C. Georgiou, K. G. Stokos, and C. N. Papanicolas, 'Engineering aspects and thermal performance of molten salt transfer lines in solar power applications', *Applied Thermal Engineering*, vol. 154, pp. 294–301, May 2019, doi: 10.1016/j.applthermaleng.2019.03.091.

[19] D. Alfani, M. Binotti, E. Macchi, P. Silva, and M. Astolfi, 'sCO2 power plants for waste heat recovery: design optimization and part-load operation strategies', *Applied Thermal Engineering*, vol. 195, p. 117013, Aug. 2021, doi: 10.1016/j.applthermaleng.2021.117013.

[20] D. Alfani, M. Astolfi, M. Binotti, P. Silva, and E. Macchi, 'Off-design performance of CSP plant based on supercritical CO2 cycles', presented at the SOLARPACES 2019: International Conference on Concentrating Solar Power and Chemical Energy Systems, Daegu, South Korea, 2020, p. 130001. doi: 10.1063/5.0029801.

[21] M. Ficili, P. Colbertaldo, S. Campanari, and G. Guandalini, 'Investigating the Partial Load of Reversible Solid Oxide Cell Systems: A Focus on Balance of Plant and Thermal Integration (Under review)', Rochester, NY, Aug. 06, 2024. Accessed: Sep. 03, 2024. [Online]. Available: https://papers.ssrn.com/abstract=4917633

[22] T. Gibson and N. Kelly, 'Optimization of solar powered hydrogen production using photovoltaic electrolysis devices', *International Journal of Hydrogen Energy*, vol. 33, no. 21, pp. 5931–5940, Nov. 2008, doi: 10.1016/j.ijhydene.2008.05.106.